Bragg reflection in a quantum periodic structure

Yueyue Chen (陈月月)[1,2], Xunli Feng (冯勋立)[3], Zhizhan Xu (徐至展)[1], and Chengpu Liu (刘呈普)[1,*]

[1]*State Key Laboratory of High Field Laser Physics, Shanghai Institute of Optics and Fine Mechanics, Chinese Academy of Sciences, Shanghai 201800, China*

[2]*University of Chinese Academy of Sciences, Beijing 100039, China*

[3]*Department of Physics, Shanghai Normal University, Shanghai 200234, China*

**Corresponding author: chpliu@siom.ac.cn*

Received August 27, 2015; accepted October 16, 2015; posted online December 10, 2015

We investigate the reflected field for few-cycle ultra-short laser pulses propagating through resonant media embedded within wavelength-scale structures. Full-wave Maxwell–Bloch equations are solved numerically by using the finite-difference time-domain method. The results show that the spectral feature of the reflected spectrum is determined by the Bragg reflection condition, and that the periodic structure of a dense atomic system can be regarded as a one-dimensional photonic crystal and even as a highly reflective multilayer film. Our study explains the suppression of the frequency shifts in the reflected spectrum based on the Bragg reflection theory and provides a method to control the frequency and frequency intervals of the spectral spikes in the reflected spectrum.

OCIS codes: 320.2250, 320.7150, 020.1335.

doi: 10.3788/COL201513.123201.

Rapid advances in nanofabrication techniques have given rise to a rich variety of periodic nanostructures[1], which provide an attractive way to control the light-matter interaction and light propagation. Meanwhile, the resonant interaction of quantum systems with a strong laser field has been a permanent hot topic over the last decades[2–4]. This is because these studies laid the foundation for current applications, such as the laser cooling of atoms[5], quantum information processing[6], and high-efficiency lasers[7]. Additionally, the study of the interaction between laser and quantum systems, which can be described by Maxwell–Bloch (MB) equations[8–17], has high methodological value. Thus, the phenomena and underlying physics of a few-cycle pulse propagating through a wavelength-scale periodic medium with resonant atoms have become the focus of interest of recent studies. A mass of questions has been addressed based on this theoretical model, such as reshaping laser pulses and frequency-shift control. With such a subwavelength structure, a single-cycle gap soliton can be generated[18], even with a chirped input laser pulse[19]. Song *et al.* replaced the atoms with an asymmetrical medium to generate a unipolar half-cycle pulse[17], which can be used to control and probe ultrafast electronic dynamics. Xie *et al.* also proved that the red shift in the reflected spectrum and the blue shift in the transmitted spectra can be suppressed if a periodic structure is used[18]. Subsequent works show that the frequency shifts obtained in the transmitted spectrum can be controlled by changing the layer thickness[20]. Previous works[17–20] have been focused on the transmitted pulse, in terms of the pulse shaping and frequency-shift controlling. However, the reflected field, which can be ignored in a diluted medium but is important for a dense medium, has not been fully studied. In this Letter, we numerically investigate the reflected fields of few-cycle pulses through a dense subwavelength periodic structure with resonant atoms. The results show that the spectral spikes appear in the reflected spectrum of the wavelength periodic structure, which actually acts as a one-dimensional photonic crystal, and that the frequencies and frequency intervals of the spectral spikes can be predicted by the Bragg reflection condition.

A few-cycle pulse propagates along the z-axis through a one-dimensional periodic structure of thin layers consisting of two-level atoms. The electric field is linearly polarized along the x-axis. We numerically solve the full-wave MB equations:

$$\begin{aligned}
\partial_t H_y &= -\frac{1}{\mu_0}\partial_z E_x,\\
\partial_t E_x &= -\frac{1}{\varepsilon_0}\partial_z H_y - \frac{1}{\varepsilon_0}\partial_t P_x,\\
\partial_t u &= -\frac{1}{T_2}u - \omega_0 v,\\
\partial_t v &= -\frac{1}{T_2}u + \omega_0 v + 2\Omega w,\\
\partial_t w &= -\frac{1}{T_1}(w - w_0) - 2\Omega w.
\end{aligned} \tag{1}$$

Here, H_y, P_x, μ_0, and ε_0 are the magnetic field, the macroscopic polarization, the permeability, and the permittivity of free space, respectively. ω_0 is the resonant frequency. T_1 and T_2 are the lifetime of the excited state and the de-phasing time, respectively. The spatial modulation of $P_x(z,t)$ is given by:

$$P_x(z,t) = \begin{cases} N d u(z,t) & z \in 2n\delta, 2(n+1)\delta], \\ 0 & z \in 2(n+1)\delta, 2(n+2)\delta], \end{cases} \tag{2}$$

where $N = 1.1 \times 10^{20}$ cm^{-3} is the medium density, $d = 2 \times 10^{29}$ A $*$ s $*$ m the dipole moment, and δ is the layer

thickness. We define a collective frequency parameter, $\omega_c = Nd^2/\epsilon_0\hbar = 0.05$ fs^{-1}, to represent the coupling strength between the medium and the field. The period of the multiple-layer system is $d = a \cdot n_a + b \cdot n_b$, where a and b (n_a and n_b) are the thicknesses (refractive index) of the atomic and the air layer, respectively. The initial electric field is defined as $\Omega(t=0,z) = \Omega_0 \cos[\omega_p(z-z_0)/c]\mathrm{sech}[1.76(z-z_0)/c\tau_p]$, where Ω_0 is the peak Rabi frequency, $\omega_p = 5$ fs is the FWHM, $\omega_p = 2.3$ fs^{-1} is the carrier frequency, and $z_0 = 26.25$ μm used to avoid the initial disturbance from the input pulse. The corresponding envelope area is $A = \Omega_0\tau_p\pi/1.76 = 2\pi$.

First, we model few-cycle pulse propagation through a periodic structure with $\delta = \lambda_0/2$. The corresponding MB equations can be solved by Yee's finite-difference time-domain discretization method for the electromagnetic fields[21,22] and the predictor-corrector method for the medium variables[9,23]. The results are shown in Fig. 1. It can be seen that the reflected field consists of a leading part and a long tail. The leading part corresponds to the reflections from each layer, while the long tail corresponds to the emission of the energy that resides in the medium after the pulse leaves. The reflected spectrum in Fig. 1(b) consists of two strong spikes located at $\omega = 0.55\omega_0$ and $\omega = 1.45\omega_0$, and weak spikes near the resonance frequency. The respective Fourier transformations of the leading part and the tail in Fig. 1(a) show that the two strong spikes come from the interference of the reflections, while the weak spikes come from the emission.

Next, we elaborate the formation of the interference constructive spikes in the reflected spectrum. The considered periodic medium can be regarded as a one-dimension photonic crystal with $d = a \cdot n_a + b \cdot n_b = \delta(n_a + 1)$. Any photon with a wavelength located in the photonic band gaps ($kd = m\pi, m = 1, 2, 3\ldots$) is forbidden to propagate through the medium, thus forming the spectral spikes in the reflected spectrum. The origin of the spectral spikes can also be understood as a Bragg reflection, where a photon with a frequency that fulfills $2d = m\lambda (m = 1, 2, 3\ldots)$ is totally reflected by the periodic medium. Thus, for a periodic structure with $\delta = \lambda_0/2$, the spectral spikes are expected to appear at $\omega_m = m\omega_0/n_a(\omega_m)(n_a(\omega_m)+1)$ $(m = 1, 2, 3\ldots)$, which is consistent with the spectral features of Fig. 1(b). Specifically, two strong spikes that appeared in Fig. 1(b) correspond to $\omega_1 = \omega_0/n_a(\omega_1)(n_a(\omega_1)+1)$ and $\omega_3 = 3\omega_0/n_a(\omega_3)(n_a(\omega_3)+1)$. However, the resonance frequency component $\omega_2 = 2\omega_0/n_a(\omega_2)(n_a(\omega_2)+1) \approx \omega_0$ disappears in the reflected spectrum due to the large absorption caused by the resonance medium. The refractive index $n_a(\omega)$ of this system can be obtained as follows.

$P(\omega) = Ndu(\omega) = \epsilon_0\chi(\omega)E(\omega)$, where $P(\omega)$ and $E(\omega)$ are the complex amplitude of the polarization and electric fields in the frequency domain, respectively. $\chi(\omega)(\chi(\omega) = \chi_L(\omega) + \chi_{NL}(\omega))$ characterizes both the linear and nonlinear behaviors of the system considered[9]. The susceptibility takes the form $\chi(\omega) = \frac{Ndu(\omega)}{\epsilon_0 E(\omega)} = \omega_c \frac{u(\omega)}{\Omega(\omega)}$, and the refractive index is $n(\omega) = \mathrm{Re}\sqrt{1+\chi(\omega)} = \frac{1}{\sqrt{2}}(((1+\chi')^2 + \chi'')^{1/2} + (1+\chi'))^{1/2}$. The real parts of the susceptibility and refractive index as functions of the frequency are shown in Fig. 2(b). It can be seen that $n(\omega_0) \approx 1$, and that $n(\omega)$ is proportional to ω near the resonance frequency ω_0, which is the case of normal dispersion. Thus, $n(\omega) < 1$ for red detuning and $n(\omega) > 1$ for blue detuning. The frequency of the spectral spike on the red side of the reflected spectrum satisfies $\omega_1 = \omega_0/n(\omega_1)(n(\omega_1)+1) > 0.5\omega_0$, while on the blue side, $\omega_3 = \omega_0/n(\omega_3)(n(\omega_3)+1) < 1.5\omega_0$, which is consistent with the reflected spectrum shown in Fig. 1(b). Therefore, both the spectral spikes near $0.5\omega_0$ and $1.5\omega_0$ slightly shift towards ω_0 due to the dispersion characteristic of the medium.

For the resonance medium discussed above, the interaction between laser and matter is strong, while for a large detuning medium, the interaction weakens and fulfills the condition of the weak excitation limit. Thus, if the resonance medium is replaced by a large detuning medium, the shifts of the spectral spike are expected to change

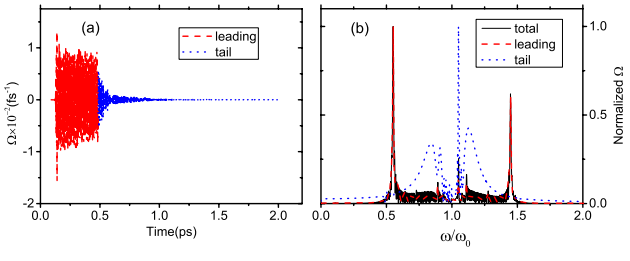

Fig. 1. (a) Reflected field and (b) spectrum of a pulse with $A = 2\pi$, $\tau_p = 5$ fs incident on a periodic structure with $\delta = \lambda_0/2$, $L = 45$ μm and $\omega_c = 0.05$ fs^{-1}. The dashed and dotted lines correspond to the leading and tail parts of the reflected fields, respectively.

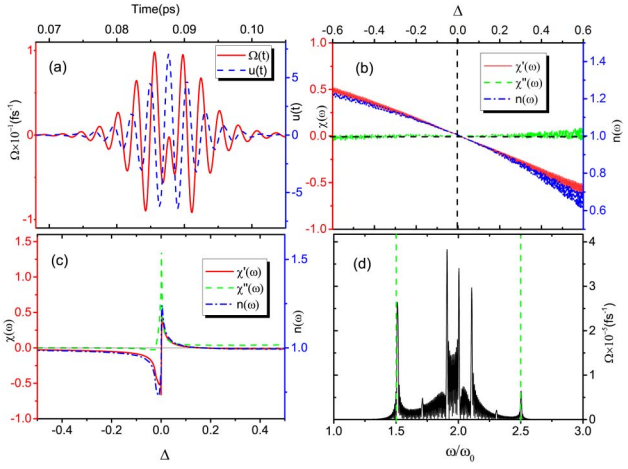

Fig. 2. (a) Time evolution of $\Omega(t)$ and $u(t)$ in a resonance medium with $\omega_p = \omega_0$. (b) The changing curves of χ', χ'', and n versus Δ in the case of (a). (c) Same as that for (b), but for a detuning medium with $\omega_p = 2\omega_0$. (d) The reflected spectrum under the same parameters as (c). The other parameters are same as those in Fig. 1.

as a result of the variation of the medium dispersion characteristic. For a detuning medium such as $\omega_p = 2\omega_0$, the change laws of $\chi(\omega)'$ and $\chi(\omega)''$ and $n(\omega)$ versus ω go back to the ordinary description of the dispersion characteristic of the two-level atomic system in quantum optics, as shown in Fig. 2(c). In ordinary quantum optics[2], under the slowly varying envelope approximation and rotating-wave approximation, the polarization takes the form $P(t) = -\frac{Nd^2}{\hbar} E(t) \frac{\rho_{aa}(t)-\rho_{bb}(t)}{(\omega_0-\omega)-i\gamma_2}$. In the limit of the weak medium excitation $\rho_{aa}(t) - \rho_{bb}(t) = \rho_{aa}(0) - \rho_{bb}(0) = -1$, the polarization is simplified to $P(t) = \varepsilon_0 E(t) \frac{\omega_c}{\Delta - i\gamma_2}$, where Δ denotes the detuning between the atomic resonance frequency and the laser frequency, $\Delta = \omega_0 - \omega$. Thus, the susceptibility is $\chi(\omega) = \frac{\omega_c}{\Delta - i\gamma_2}$ and the refractive index $n(\omega) = \mathrm{Re}\sqrt{1 + \frac{\omega_c}{\Delta - i\gamma_2}}$. As shown in Fig. 2(c), both $\chi(\omega)'$ and $n(\omega)$ are inversely proportional to ω near the resonance frequency ω_0, and are accompanied by strong absorption ($\chi(\omega)'' > 0$). This is the case of abnormal dispersion. The reflected spectrum for the detuning medium is shown in Fig. 2(d). It can be seen that the interference spikes appear at $1.5\omega_0$ and $2.5\omega_0$, which correspond to $\omega_3 = 3\omega_0/n_a(\omega_3)(n_a(\omega_3)+1)$ and $\omega_5 = 5\omega_0/n_a(\omega_5)(n_a(\omega_5)+1)$ predicted by the interference theory, respectively. The shift of the spike from $1.5\omega_0$ in Fig. 1(b) vanishes in Fig. 2(d), since for the latter, $n(\omega_m) \approx 1 (m = 3, 5)$, as shown in Fig. 2(c). In addition, the slight shift in Fig. 2(d) is away from ω_0 because both the spikes are on the blue side of the spectrum and $n(\omega) < 1$ for $\Delta < 0$. Therefore, the location of the spike in the reflected spectrum is determined by the dispersion characteristic of the medium, which is affected by the detuning between the carrier frequency of laser and the atomic transition frequency.

We then turn to another spectral feature of the reflected spectrum, the frequency intervals of the spectral spikes. We further model the few-cycle pulse propagation through various periodic structures with $\delta = k\lambda_0 (k = 2, 1, 1/4)$. The frequency intervals are labeled in the reflected spectra, as shown in Fig. 3. According to the Bragg reflection condition, the frequency interval $\Delta\omega \approx \omega_0/2n_a(n_a+1)k \approx 0.25\omega_0/k (k = 2, 1, 1/4)$. For example, when $k = 2$, the frequency interval is $\Delta\omega \approx 0.1\omega_0$. The frequency interval obtained from the numerical results in Fig. 3(a) is $\Delta\omega \approx 0.1\omega_0$, which is consistent with the prediction from the above Bragg condition. Further demonstrations indicate that the consistency remains for the cases of $k = 1$ and $1/4$ (not shown here). Therefore, regarding the few-cycle pulse propagation through a periodic atomic medium, the frequency interval of the spikes in the reflected spectrum can be predicted by the Bragg reflection condition. This holds true even if laser and medium parameters change.

Figure 4 shows the reflected spectra for $A = 4\pi$, $\omega_c = 0.2$ fs^{-1} and $L = 150$ μm. When $k > 1/4$, the spectra still reserve the reflected field profile of a bulk medium. That is, most of the energy is located on the red side around $\omega = 0.65\omega_0$, as shown in Fig. 4(a). When $k < 1/4$, the major red shift is suppressed and a dominant blue shift spike appears, as shown in Fig. 4(e). This is because with the increase of the thickness of each layer, the periodic medium gradually changes to a bulk medium. The relatively small frequency interval ensures that the red shift corresponding to the bulk reflection is visible. While with the decrease of the thickness, the frequency interval increases and fewer spikes appear in the reflected spectrum. Only the spike near the center frequency and satisfying Bragg condition is visible, which corresponds to the dominant blue shift. When $k = 1/4$, both the red shift and blue shift are largely suppressed due to Bragg condition. Moreover, from the numerical results shown in Figs. 4(a)–4(e), the variance of the frequency interval $\Delta\omega$ versus k can be obtained. The result is shown in Fig. 4(f), which is consistent with the prediction of the Bragg reflection condition $\Delta\omega \approx 0.25\omega_0/k$. Note that, when it comes to few-cycle pulse propagation through a periodic medium, the suppression of the red shift in the reflected spectrum has been attributed to the breakdown of the phase-matching condition for intrapulse four-wave mixing[15]. However, based on the above discussion, we conclude that the suppression of the red shift can also be explained by the Bragg reflection theory.

Finally, we turn to the case where the optical thickness of each layer is exactly the same, $a \cdot n_a = b \cdot n_b = \delta$. The periodic medium is equal to a highly reflective multilayer film. In this case, the frequency of the spectral spikes is determined by the constructive interference condition, $2\delta + \lambda/2 = m\lambda (m = 1, 2\ldots)$. For a periodic medium where $\delta = k\lambda_0$, $\omega_m = m/4kn_a (m = 1, 3, 5\ldots)$. The equality of

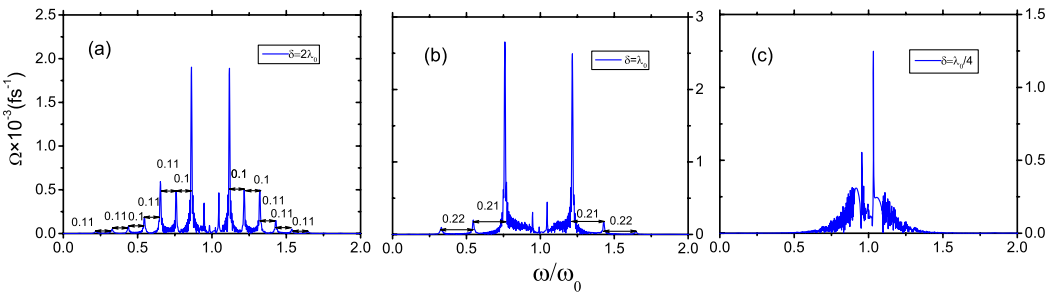

Fig. 3. $A = 2\pi$, $\tau_p = 5$ fs, $L = 45$ μm, $\omega_c = 0.05$ fs^{-1}. The reflected spectra of the periodic structures with $\delta = k\lambda_0 (k = 2, 1, 1/4)$.

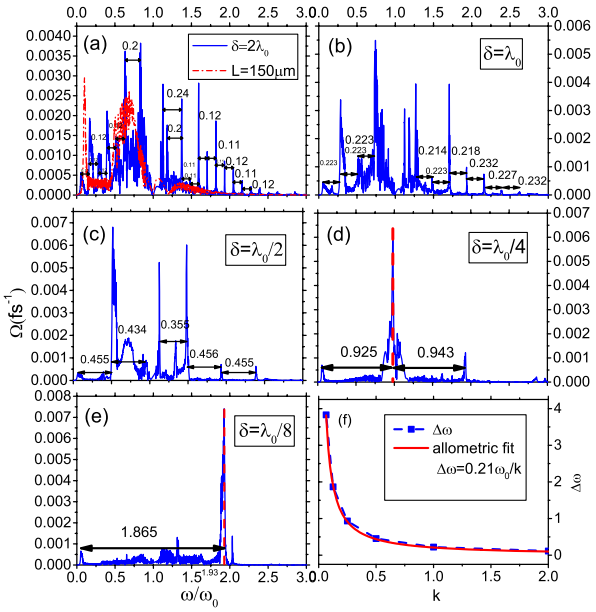

Fig. 4. (a)–(e) The reflected spectra of the periodic structures with $\delta = k\lambda_0 (k = 2, 1, 1/2, 1/4, 1/8)$. $A = 4\pi$, $\omega_c = 0.2$ fs^{-1}, $L = 150$ μm. The other parameters are same as Fig. 3. The dashed line in (a) indicates the reflected spectrum of a bulk medium. (f) The scaling law of the frequency intervals of the spectral spikes against k.

each layer ensures that destructive interference occurs for the photon with $\omega_m = m/4kn_a (m = 2, 4, 6\ldots)$. The frequency interval in this case is $\Delta\omega' = \omega_0/2n_a k \approx 0.5\omega_0/k$. Compared with the ordinary periodic medium, the frequency interval of the highly reflective film is doubled, $\Delta\omega' = 2\Delta\omega$. Since the inequality of the optical thickness of each layer ($a \cdot n_a \neq b \cdot n_b$) is responsible for the decrease of the frequency interval, the ordinary periodic medium discussed above can turn into a highly reflective film when the difference between $a \cdot n_a$ and $b \cdot n_b$ disappears. Specifically, the spectral spike located at $\omega_m = m/4kn_a (m = 2, 4, 6\ldots)$ disappears and the frequency interval changes from $\Delta\omega$ to $\Delta\omega'$. To verify these claims, we reduce the medium density to make sure the optical thickness of atomic layer $a \cdot n_a$ gets closer to that of the air

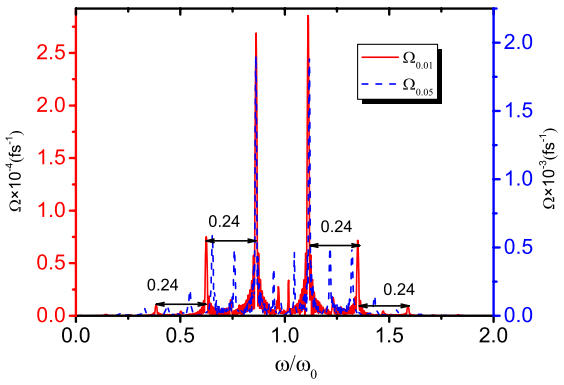

Fig. 5. Comparison of the reflected spectra of $\omega_c = 0.01$ fs^{-1} (solid line) and $\omega_c = 0.05$ fs^{-1} (dashed line).

layer, b. Take $k = 2$ as an example, as shown in Fig. 5, when the medium density decreases from $\omega_c = 0.05$ fs^{-1} to $\omega_c = 0.01$ fs^{-1}, the amplitudes of the spectral spikes located at $0.75\omega_0$ and $1.2\omega_0$ significantly decrease and the frequency interval changes from $0.11\omega_0$ to $0.24\omega_0$.

In conclusion, we numerically study few-cycle pulse propagation through a wavelength periodic structure consisting of dense two-level atoms. The results show that the medium acts as a one-dimensional photonic crystal and the spectral features of the reflected spectrum can be predicted by the Bragg reflection theory. Spectral spikes appear in the reflected spectrum. Its frequency depends on the Bragg condition and changes with the medium dispersion characteristic, which is determined by the strength of the light-matter interaction. For a strong interaction case, the spectral spikes on the blue side move towards the resonance frequency ω_0 as a consequence of the normal dispersion near ω_0. On the contrary, for a weak interaction case, the spectral spikes move away from the ω_0 due to anomalous dispersion. Moreover, the frequency interval of the spectral spikes is inversely proportional to the thickness of each layer. For $\delta = 2\lambda_0$, the reflected spectrum of the periodic medium still reserves the spectrum profile of a bulk medium, which has a large red shift due to intrapulse four-wave mixing. With the decrease of the layer thickness, the major red shift is replaced by a blue shift spike. Especially when $\delta = \lambda_0/4$, both the frequency shifts are suppressed, which is consistent with the prediction of the Bragg reflection condition. Moreover, the periodic atomic medium can simulate a highly reflective film when the optical thickness difference between each layer is removed. Thus, our study in the reflected spectrum is helpful in creating a complete picture for understanding a few-cycle pulse's propagation in a periodic quantum system. It provides a reliable tool to control the frequency and frequency intervals of the spectral spikes in the reflected spectrum, and lays the basis for simulating a photonic crystal and a highly reflective multi-layer film within a two-level atomic system.

This work was supported by the National Natural Science Foundation of China under Grant Nos. 11374318 and 11374315. C.L. is appreciative of the support from the 100-Talents Project of the Chinese Academy of Sciences and the Department of Human Resources and Social Security of China.

References

1. K. Busch, G. V. Freymann, S. Linden, S. F. Mingaleev, L. Tkeshelashvili, and M. Wegener, Phys. Rep. **444**, 101 (2007).
2. W. Yang, S. Gong, Y. Niu, and Z. Xu, Chin. Opt. Lett. **3**, 435 (2005).
3. B. Liu, S. Gong, X. Song, and S. Jin, Chin. Opt. Lett. **3**, 278 (2005).
4. H. Yao, Y. Niu, Y. Peng, and S. Gong, Chin. Opt. Lett. **10**, 011901 (2012).
5. M. O. Scully and M. S. Zubairy, *Quantum Optics* (University Press, 2001).
6. A. Blais, R. Huang, A. Wallraff, S. M. Girvin, and R. J. Schoelkopf, Phys. Rev. A **69**, 062320 (2004).

7. D. Bimberg, M. Grundmann, and N. N. Ledentsov, *Quantum Dot Heterostructures* (Wiley, 1999).
8. H. Leblond and D. Mihalache, Phys. Rep. **523**, 61 (2013).
9. R. W. Ziolkowski, J. M. Arnold, and D. M. Gogny, Phys. Rev. A **52**, 3082 (1995).
10. M. Wegener, *Extreme Nonlinear Optics* (SpringerVerlag, 2005).
11. S. Hughes, Phys. Rev. Lett. **81**, 3363 (1998).
12. O. D. Mücke, T. Tritschler, M. Wegener, U. Morgner, and F. X. Kärtnerand, Phys. Rev. Lett. **87**, 057401 (2001).
13. V. P. Kalosha and J. Herrmann, Phys. Rev. Lett. **83**, 544 (1999).
14. D. V. Novitsky, Phys. Rev. A **86**, 063835 (2012).
15. W. Yang, X. Song, S. Gong, Y. Cheng, and Z. Xu, Phys. Rev. Lett. **99**, 133602 (2007).
16. N. Cui and M. A. Macovei, New J. Phys. **14**, 093031 (2012).
17. X. Song, W. Yang, Z. Zeng, R. Li, and Z. Xu, Phys. Rev. A **82**, 053821 (2010).
18. X. T. Xie and M. A. Macovei, Phys. Rev. Lett **104**, 073902 (2010).
19. L. Guo, X. Xie, and Z. Zhan, Chin. Phys. B **22**, 094212 (2013).
20. X. Song, M. Yan, M. Wu, Z. Sheng, Z. Hao, C. Huang, and W. Yang, J. Opt. **17**, 055503 (2015).
21. K. S. Yee, IEEE Trans. Antennas Propag. **14**, 302 (1996).
22. A. Taflove and M. E. Brodwin, IEEE Trans. Microwave Theory Tech. **23**, 623 (1975).
23. Y. Chen, X. Feng, and C. Liu, Opt. Express **23**, 240039 (2015).